摩擦学学报
TRIBOLOGY

马氏体钢表面磁控溅射类金刚石薄膜滚动接触疲劳失效机理

赵凤平，李淑欣，蒲吉斌，王海新，蒋港辉

Failure Mechanism of Rolling Contact Fatigue of Magnetron-Sputterred DLC Film on Martensite Steel

ZHAO Fengping, LI Shuxin, PU Jibin, WANG Haixin, JIANG Ganghui

在线阅读 View online: https://doi.org/10.16078/j.tribology.2020244

第 42 卷　第 1 期
2022 年 1 月

摩 擦 学 学 报
Tribology

Vol 42　No 1
Jan, 2022

DOI: 10.16078/j.tribology.2020244

马氏体钢表面磁控溅射类金刚石薄膜滚动接触疲劳失效机理

赵凤平[1], 李淑欣[1*], 蒲吉斌[2], 王海新[2], 蒋港辉[1]
(1. 宁波大学 机械工程与力学学院, 浙江 宁波 315211;
2. 中国科学院 宁波材料技术与工程研究所 海洋功能材料实验室, 浙江 宁波 315201)

摘　要: 采用磁控溅射技术在马氏体钢基体表面制备类金刚石(DLC)薄膜，应用扫描电镜、Raman光谱仪和划痕测试仪等对薄膜进行表征. 基于对失效表面及截面微观特征的详细分析，研究了DLC薄膜在接触疲劳载荷下的失效特征和机理. 结果表明：DLC薄膜试样的滚动接触疲劳(RCF)寿命比基体的寿命显著提高，且薄膜磨损后试样的剩余寿命仍比原基体寿命长. 薄膜厚度3 μm，处于接触最大应力分布的15 μm范围内. DLC薄膜是从基体表面粗糙峰处产生微裂纹进而导致薄膜剥落，基体材料裸露，最终试样失效.

关键词: 类金刚石薄膜; 磁控溅射; 马氏体钢; 滚动接触疲劳; 失效机理
中图分类号: TH117.1　　**文献标志码:** A　　**文章编号:** 1004-0595(2022)01–0153–10

Failure Mechanism of Rolling Contact Fatigue of Magnetron-Sputterred DLC Film on Martensite Steel

ZHAO Fengping[1], LI Shuxin[1*], PU Jibin[2], WANG Haixin[2], JIANG Ganghui[1]

(*1. School of Mechanical Engineerying and Mechanics, Ningbo University, Zhejiang Ningbo 315211, China*
2. Laboratory of Marine Functional Materials, Ningbo Institute of Materials Technology and Engineering, Chinese Academy of Sciences, Zhejiang Ningbo 315201, China)

Abstract: Bearing is one of the key components in mechanical system. Rolling bearings normally fail in the way of surface pits and spalling due to rolling contact fatigue (RCF). Compared to the conventional fatigue failure, the RCF failure is more complicated, involving wear, mulitiaxial fatigue loading, phase transformation in subsurface material, and many others. This leads to the practical service life of bearings much shorter than the designed life. Therefore, improving the resistance to rolling contact fatigue and wear is a big challenge among industries and academia. Surface technology is one of the effective solutions for improvement of surface quality. Diamond-like carbon (DLC) film is a kind of amorphous carbon film similar to diamond. It has low friction coefficient, high hardness, small thermal expansion coefficient and good wear resistance. Extensive investigations have been conducted on DCL film regarding mechanical and tribological properties, such as elastic modulus improvement, adhesive wear resistance, frictional dependence of grapheme and influential factors. However, there has been a very limited work on RCF. And these reported studies focused on fatigue life and failure on macro scale. The failure mechanism and some typical micro scale failure features of DCL film have not yet been well understood. In this study, the DLC film was successfully prepared on martensitic steel using magnetron sputtering technique. RCF tests were carried out for samples with and without DLC film under

Received 3 November 2020, revised 10 February 2021, accepted 17 February 2021, available online 20 February 2021.
*Corresponding author. E-mail: lishuxin@nbu.edu.cn, Tel: +86-574-87609954.
This project was supported by the Natural Science Foundation of China (52075271, 51675287) and K C Wong Magna Fund in Ningbo University.
国家自然科学基金项目(52075271，51675287)和宁波大学王宽诚幸福基金资助.

lubrication on a two-roller machine. The failure mechanism was investigated based on the detailed analysis of surfaces and sections of failed specimens. The failed surfaces and sections morphologies were inspected by using scanning electron microscope. The Raman spectra of the film was characterized by 2000 micro-Raman system. Energy dispersive spectrometer was used to observe the element distribution between DLC film and substrate. The bonding strength between the film and substrate was measured by a scratch tester. The nano hardness and elastic modulus of the film were measured by nano indentation tester. The experimental results showed that the DLC film on the surface of martensitic steel displayed a high hardness and elastic modulus, and a high interfacial bonding strength between the DLC film and the substrate. The DLC film can significantly improve the RCF life. Furthermore, the samples with the DLC worn out showed even longer residual lives compared to the uncoated samples. On the one hand, it was due to the high hardness of the DLC film itself. On the other hand, a carbon-containing transfer film was formed during the repetitious rolling contact process of the DLC film. The transfer film had graphitization characteristics, which acted as a certain lubrication role. The RCF performance of the DLC film samples was influenced by the surface roughness peak of the substrate, contact pressure, sliding ratio, among which the surface roughness peak showed the biggest influence. The thickness of the DLC film was 3 μm, within the range of 15 μm of the maximum stress distribution. Under cyclic contact stress, the micro cracks initiated preferentially at surface roughness peak and resulted in film spalling. With the increasing number of cycles, the film was worn out and the base material was exposed. A large plastic deformation and micro cracks were generated in the surface and subsurface of base material under RCF, which eventually led to surface pits and material spalling.

Key words: diamond-like carbon film; magnetron sputtering; martensitic steel; rolling contact fatigue; failure mechanism

轴承作为机械设备中关键的滚动零部件，其寿命和可靠性将直接影响整个工作系统的稳定. 轴承在接触疲劳载荷下，接触表面产生裂纹导致材料剥落形成微小点蚀. 对失效的轴承内圈截面分析发现，在亚表面分布着大量深度在1 mm以内的微裂纹，这些微裂纹是产生疲劳点蚀的根源[1]. 因此，通过表面技术改善抗接触疲劳和磨损性能，是提高轴承寿命的主要途径之一[2]. 类金刚石(Diamond-like carbon，DLC)薄膜是一类硬度、光学、电学和摩擦学等特性类似于金刚石的非晶碳膜. 具有摩擦系数低、硬度高、弹性模量大、热导率高、热膨胀系数小及耐磨性好等独特的性能，能够显著改善材料的摩擦、磨损和疲劳行为[3-7]. 国内外学者对类金刚石薄膜的摩擦学特性[8-12]做了大量工作，但对DLC薄膜接触疲劳性能的研究工作主要集中在接触疲劳寿命和宏观机械性能方面[13-16]，而缺乏对微观失效特征和机理的研究. 本文作者以马氏体钢为试验对象，应用Teer CF-800封闭场非平衡磁控溅射装置制备类金刚石薄膜，使用MJP-30型滚动接触疲劳试验机进行滚动接触疲劳(RCF)试验，研究DLC薄膜样品的滚动接触疲劳行为及失效机理，为类金刚石薄膜在接触疲劳等方面的应用提供理论依据.

1 试验部分

1.1 试样与薄膜制备

试验原材料选用GCr15轴承钢，其热处理工艺是在860 ℃下保温2 h，待其全部奥氏体化后油淬至室温，然后在160 ℃保温1 h，得到回火马氏体组织，化学成分(质量分数)主要为Fe，其他元素质量分数分别为0.90% C、0.32% Mn、1.87% Cr、0.31% Si、0.02% S和0.027% P. 滚动接触疲劳试样根据YB-T5345-2006设计，主试样和陪试样的直径均为60 mm，接触宽度为5 mm，基体试样接触表面的平均粗糙度R_a为0.8 μm，试样形状如图1所示[17].

(a)

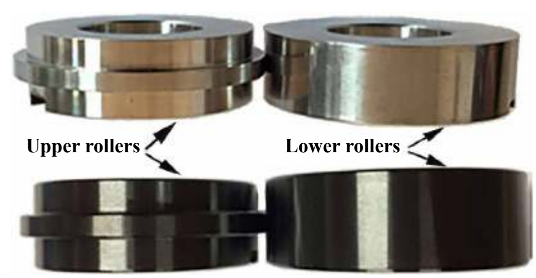

(b)

Fig. 1 Photo of the samples in RCF for (a) substrate samples and (b) DLC film samples

图 1 RCF试验样品示意图：(a)基体试样；(b)DLC薄膜试样

薄膜样品制备均采用Teer CF-800封闭场非平衡磁控溅射装置. 镀膜前所有试样均进行机械抛光，在丙酮和无水乙醇中各超声清洗20 min，然后用氮气吹干以防止试样表面污染，形成清洁的表面. 清洗吹干后放入烘箱内进行烘干，之后放入真空室. DLC薄膜沉积的详细步骤如下：首先，预抽真空至3.0×10^{-3} Pa以下，

通入质量分数为99.99%的氩气，氩气流量为30 sccm，调节脉冲偏压电源电压值为−500 V，进行氩等离子体对基底表面轰击清洗30 min. 其次，将偏压调至−70 V，在基底表面沉积Cr过渡层，厚度约0.3 μm. 随后，逐渐减小Cr靶溅射功率(200~0 W)并使C靶功率(3~4 kW)与WC靶功率(100~300 W)增加至预设值，制备梯度过渡层及表面碳膜，薄膜厚度约3 μm.

1.2　薄膜性能测试

使用日立SU-5 000型扫描电子显微镜(SEM)测定薄膜厚度并观察薄膜的微观结构和试样的失效表面形貌；使用2000 micro-Raman系统采集薄膜的拉曼光谱；使用能谱仪(EDS)观察DLC薄膜与基底之间的元素分布；使用划痕试验仪测定薄膜同基体的结合强度，划痕载荷由0 N增至60 N，划痕长度3 mm；采用纳米压痕试验机对薄膜的纳米硬度和弹性模量进行了测定. 为减少试验的不确定性，在不同位置进行重复测试，取平均值.

1.3　接触疲劳试验

采用MJP-30型滚动接触疲劳试验机，在油润滑的条件下研究材料的接触疲劳性能. 最大赫兹接触应力为1.8和2.4 GPa，滑差率为5%和15%. 当被测试样表面发生失效导致试验机振动水平超过预设值时，试验停止. 试样分为两组：第一组试样未镀膜，为基体试样；第二组试样为DLC薄膜试样. 由于滚动接触疲劳寿命存在较大的离散性，为了得到统计结果，在每种试验条件下进行了3次滚动接触疲劳试验. 试验后，所有样品用丙酮进行超声波清洗，然后用电火花线切割机将试样沿圆周和轴向方向制备成近似长方体的样品，将切割好的样品进行研磨并机械抛光，之后用5%硝酸酒精溶液浸泡腐蚀，腐蚀完后先用去离子水冲洗干净，再用无水乙醇进行超声波清洗，取出用热风吹干，将接触疲劳试验后的试样进行表面及截面的特征分析.

2　结果与讨论

2.1　DLC薄膜的表面与截面形貌

图2为GCr15马氏体钢基体上磁控溅射的DLC薄膜微观形貌，从图2(a)中可以看出，薄膜表面存在少量孔隙，无明显的未融颗粒、层间裂纹等微观缺陷. 由于基体表面不平整(R_a=0.8 μm)，致密性不够，导致所制备薄膜表面出现孔隙. 图2(b)为DLC薄膜的截面形貌图，可以看出DLC薄膜与基体的结合状态良好，薄膜厚度约为3 μm，过渡层厚度约为0.3 μm. 图2(c)为DLC薄膜沿截面深度方向的EDS元素成分及分布信息图，可以清晰地观察到DLC薄膜的化学成分主要为C、Ar和W等，过渡层的主要成分为Cr.

2.2　薄膜力学性能

轴承钢基体试样的硬度为630±10 HV. 通过纳米压痕试验机测得DLC薄膜的纳米硬度为22.4 GPa，弹性模量为257.8 GPa. 图3为纳米压痕试验中DLC薄膜的载荷-位移曲线. 在一定的硬度范围内，DLC薄膜抗接触疲劳性能随硬度的增大而升高[18].

划痕试验通常用于评价薄膜同基体之间的结合强度，图4(a)示出了DLC薄膜试样典型划痕形貌光学显微照片. 可以看出，从划痕开始到划痕结束，随着载荷的增大，表面划痕逐渐变宽加深. 如图4(b)所示，在30 N左右划痕内部可以观察到大量裂纹，但未出现薄膜失效迹象. 在60 N高载荷作用下，划痕末端出现明显的剥落和裂纹，划痕内部薄膜失效，如图4(c)所示. 由上述现象可得出，马氏体钢基体表面的DLC薄膜的临界载荷较高[19-21](大于50 N). 其原因在于DLC薄膜自身硬度较高，力学性能好，且Cr过渡层具有优异的耐磨性，同时能与马氏体钢基体良好的结合[21-23]. 高的临界载荷有利于延缓薄膜的失效，提高薄膜的使用寿命[19].

2.3　滚动接触疲劳性能

图5为载荷和滑差率分别为1.8 GPa-5%、1.8 GPa-15%和2.4 GPa-15%条件下DLC薄膜和基体的接触疲劳寿命试验结果. 每个数据点是3个试样寿命的平均值. 其中，红色和蓝色表示DLC薄膜试样的寿命，红色表示薄膜磨掉以后裸露基体的剩余寿命，绿色表示未镀膜的基体试样寿命. 与基体试样相比，DLC薄膜试样的接触疲劳寿命明显提高. 载荷和滑差率越大，寿命越短. 同时，DLC薄膜磨损完后的剩余寿命仍比基体寿命长[13]. 这是由于：一方面，DLC薄膜增加了接触表面的硬度. 在一定的硬度范围内，接触疲劳抗力随硬度的增大而升高，且Cr过渡层可以作为硬支撑层，通过增加竖向载荷的承载力减小磨损深度，进而提高接触疲劳寿命[18]；另一方面，薄膜在滚动接触过程中形成的转移膜具有石墨化特征，被磨损掉的石墨又填充到凹坑，起到一定的润滑作用，从而减少磨损[16,24].

图6(a)为所制备DLC薄膜的Raman光谱，图6(a)中所示的不对称的宽散射峰属于典型的DLC薄膜的特征拉曼峰，采用Gaussian拟合技术可将其分解成两个峰，分别为位于1 350 cm^{-1}附近的D峰和位于1 560 cm^{-1}附近的G峰[12,19]. 其中G峰的谱带由无序的石墨产生，而D峰的谱带则与细小石墨有关[24]. DLC主要由金刚石键(sp^3)和石墨键(sp^2)组成，薄膜中sp^3/sp^{2}值决定了

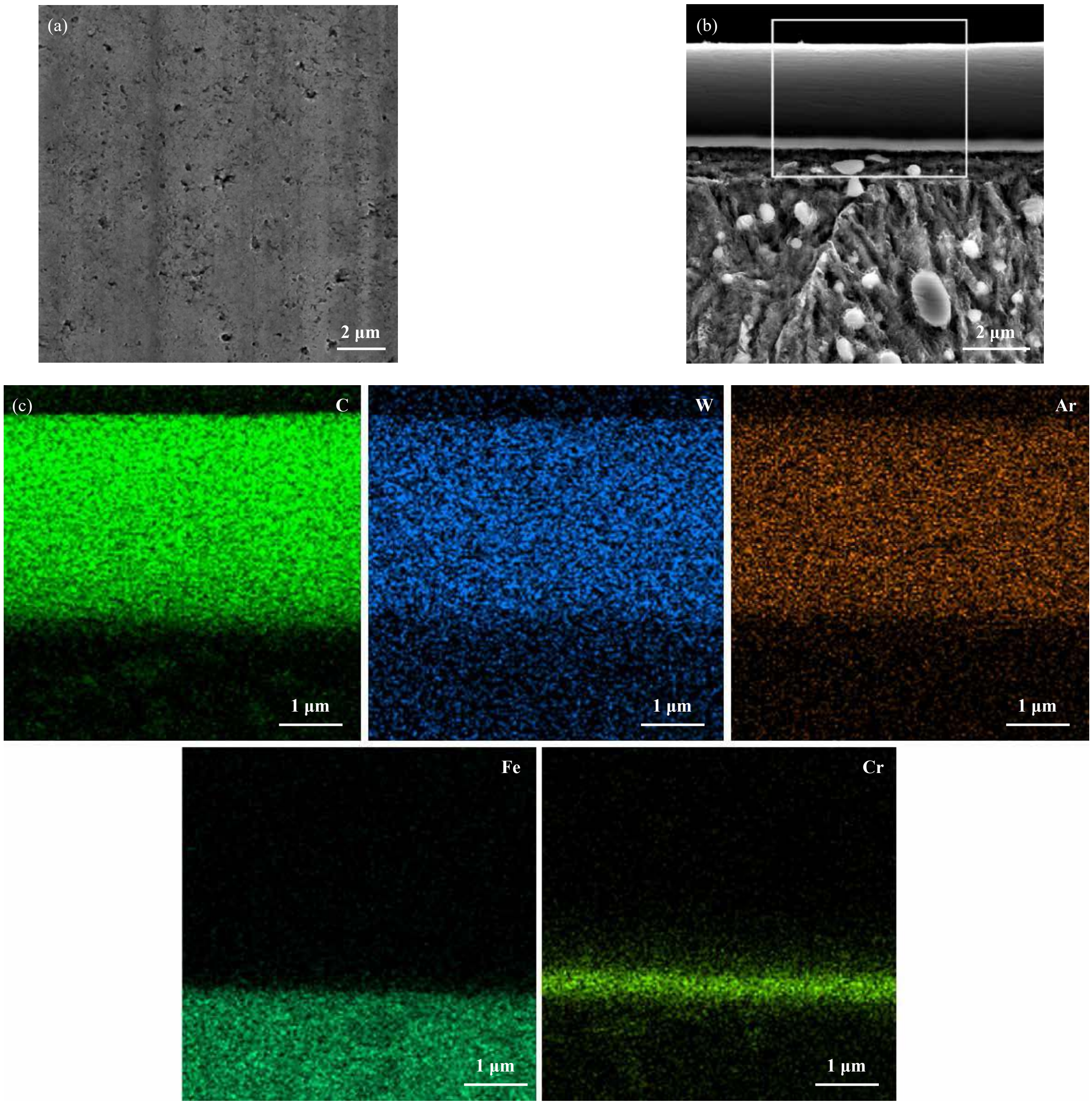

Fig. 2 Micrographs of the DLC film: (a) surface image; (b) cross-sectional image; (c) EDS scan image of the selected area in (b)
图 2 DLC薄膜的微观形貌图：(a)表面图像；(b)截面图像；(c)图(b)中选定区域的EDS扫描图像

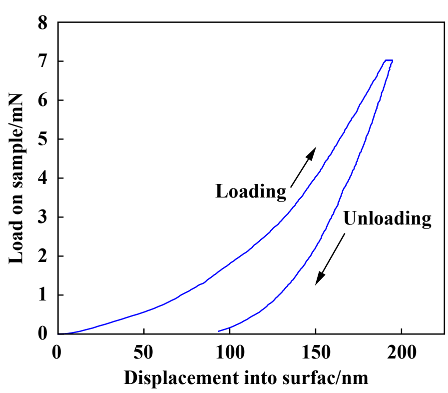

Fig. 3 Load-displacement curve of the DLC film by nanoindentation
图 3 DLC薄膜的纳米压痕载荷-位移曲线

DLC薄膜的性能. Raman光谱中D峰与G峰对应的积分强度比I_D/I_G越小，则膜中sp^3碳含量越高，在宏观性质上就越类似于金刚石[24].

经过1.2×10^5次循环后，对类金刚石薄膜进行拉曼光谱分析，试验参数：接触应力1.8 GPa，滑差率5%. 如图6(b)所示，试验后类金刚石碳膜的G峰向高频端移动[25-26]，峰的形状更接近于石墨峰，在1 350 cm^{-1}处的峰强度增加，表明石墨键的贡献增大[9]. 通过高斯函数拟合计算得出特征峰比值I_D/I_G大于1，说明此时试样表面主要是硬度相对较低的含有更多sp^2键结构的含碳转移膜[27-29]. DLC薄膜在滚动接触过程中形成的转

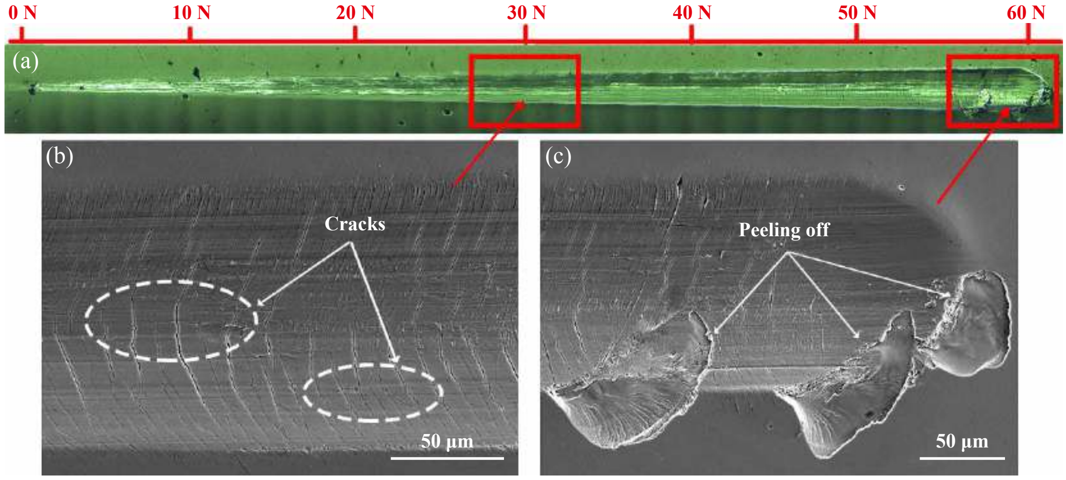

Fig. 4 Morphologies of scratch tracks for DLC film: (a) optical microscope image; (b) SEM micrograph at the load of 30 N; (c) SEM micrograph at the load of 60 N

图 4　DLC薄膜划痕形貌图：(a)光学显微照片；(b)载荷为30 N时的SEM照片；(c) 载荷为60 N时的SEM照片

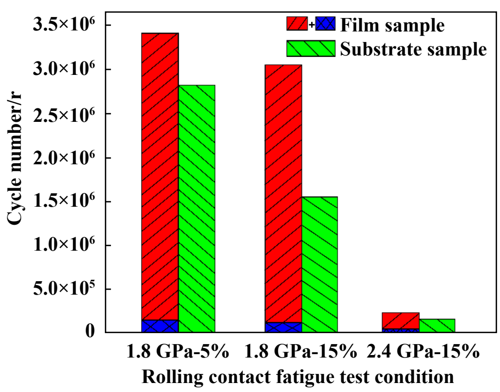

Fig. 5　Comparison on RCF life of DLC films and substrate specimens under different loads and slip rates

图 5　不同载荷及滑差率下DLC薄膜和基体试样接触疲劳寿命比较

移膜具有石墨化特征[30-32]，从而有利于提高耐磨性.

2.4　接触疲劳失效表面和横截面特征分析

图7为薄膜试样磨损表面的元素分析，试验参数：接触应力1.8 GPa，滑差率5%和循环次数为1.92×10^6. 可以看出，DLC薄膜磨损较为严重，滚道接触区存在明显的周向磨损痕迹，但接触表面仍有部分薄膜. 由上述的拉曼光谱分析可知，此时有含碳转移膜生成. 含碳转移膜的生成可以有效地避免接触面的直接接触，降低滚动接触过程中的剪切力[19]，使DLC薄膜轴承表现出较好的接触疲劳性能.

图8为不同周次DLC薄膜试样磨损表面和横截面形貌的SEM照片. 图8(a)为试验前DLC薄膜试样表面形貌图，粗糙峰均匀分布于表面，使用激光共聚焦扫描显微镜(LSCM)测得薄膜试样的平均表面粗糙度R_a为0.8 μm，与基体GCr15马氏体钢的粗糙度几乎相等. DLC薄膜基本不改变基体表面形貌，其原因在于DLC薄膜无定形的内在属性使得取向优先生长导致粗糙度增加的过程不会发生，且薄膜具有沿基底表面生长的特性，最终的粗糙度会与基体相近[21]；图8(b)为循环3×10^4周次时表面形貌图，发现试样表面的粗糙峰基本被磨损，暴露出金属基体；随着循环次数增至1.2×10^5，薄膜发生大面积剥落，基体表面出现凹痕和剥落坑[图8(c)]；继续加载至1.8×10^5周次时，薄膜几乎已被完全磨损，基体表面出现了明显的沟槽[图8(d)]. 图8(e)和(f)为接触疲劳失效过程截面形貌图，从图8(e)中可以看出薄膜呈波浪状沉积在试样表面. 在滚动接触疲劳载荷的作用下，薄膜首先从凸起的粗糙峰处开始剥落，之后向四周扩展，如图8(f)所示，并且同图8(b)所示结果一致.

2.5　失效机理分析

由赫兹接触理论，裂纹起源于距表面0.75 b的最大剪切应力处，其中b为接触圆半径. 采用有限元软件ABAQUS计算了Mises应力，如图9所示. 最大应力位于距离表面15 μm处，而DLC薄膜厚度为3 μm，因此薄膜处于最大应力分布范围内. 薄膜表面凹凸不平，由粗糙峰和粗糙谷组成[见图8(a)]，接触最先发生在粗糙峰处，较大的粗糙峰在试验过程中易导致摩擦副间接触面积减小，接触应力增大，应力集中严重[7]，且由于基体表面不平整及致密性不够导致所制备的薄膜表面存在孔隙，也是应力集中的部位，容易在粗糙峰处的孔隙边缘产生微裂纹. 在接触应力的作用下，粗糙峰处的薄膜开始剥落，金属基体裸露，接触表面产生

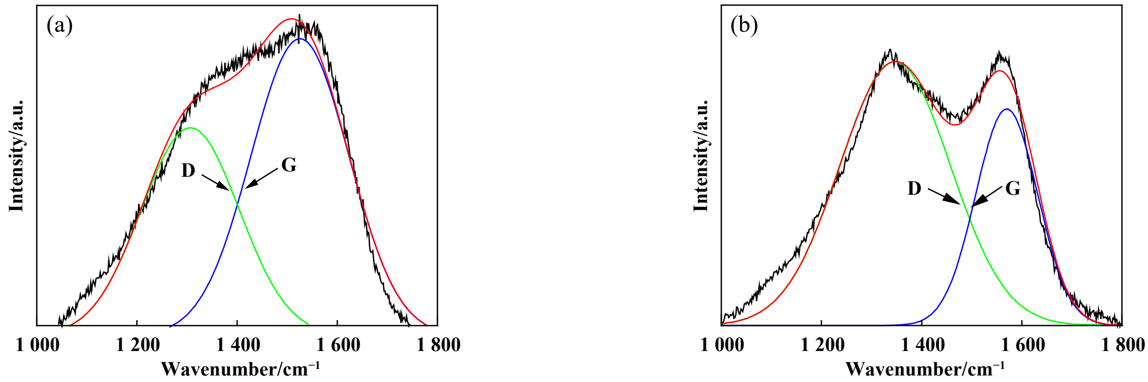

Fig. 6 Raman spectra of the DLC film: (a) before RCF testing; (b) 1.2×10^5 cycles

图 6 DLC薄膜的Raman光谱：(a)RCF试验前；(b)试验1.2×10^5周次

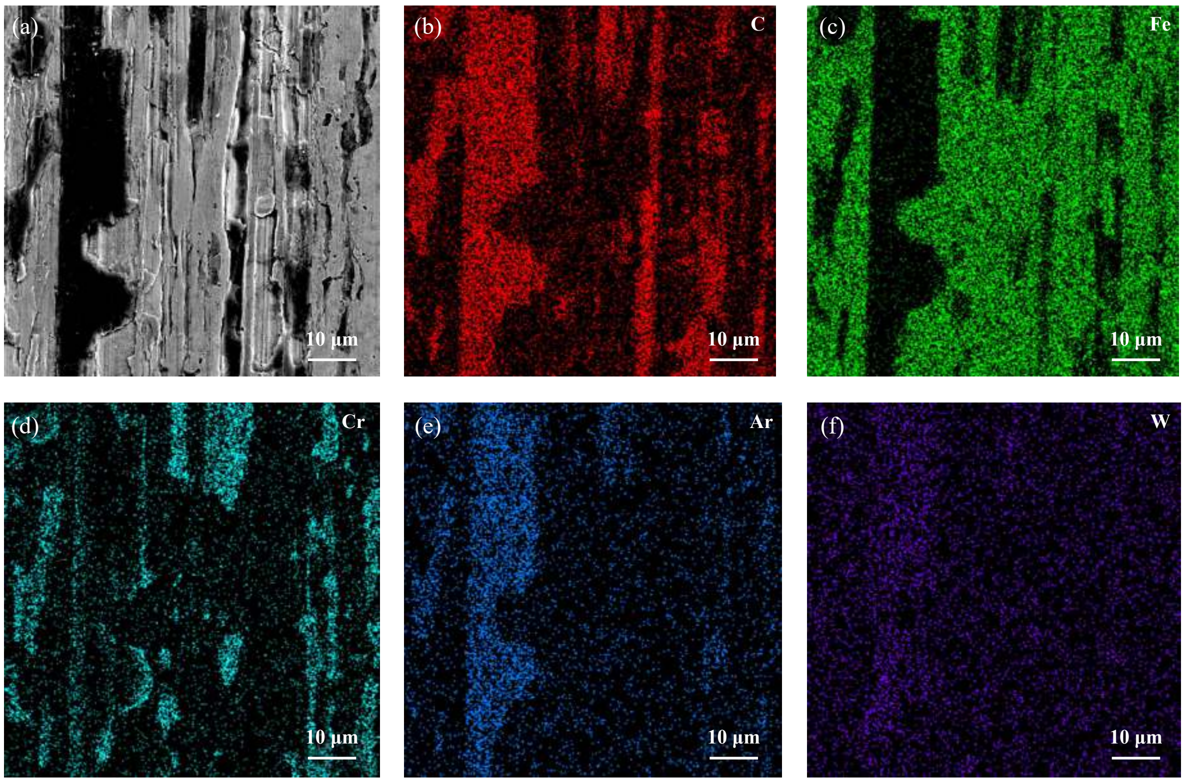

Fig. 7 Morphologies of worn surface of DLC film samples: (a) SEM micrograph; (b~f) EDS mappings of C, Fe, Cr, Ar, and W

图 7 DLC薄膜试样磨损表面显微照片：(a)SEM照片；(b~f) C, Fe, Cr, Ar 和W元素分布图

裂纹，向内扩展一定距离后转向表面，导致基体材料剥落形成点蚀坑. 大量的点蚀坑密布于接触表面，如图10(a~b)所示. 随着继续加载，相邻的点蚀坑互相连接，形成面积较大且较深的剥落坑，其深度大约为1 mm，如图10(c)所示. 随着循环次数的增加，当薄膜磨完后，基体在疲劳载荷的作用下产生大量塑性变形和疲劳裂纹，最终导致试样失效，如图10(d~e)所示.

图11为DLC薄膜试样的滚动接触疲劳失效机理示意图. 首先，在循环载荷的作用下，接触表面出现较浅的磨痕，试样表面生成硬度相对较低的含有更多sp^2键结构的含碳转移膜；然后，随着循环次数的增加，薄膜剥落，基体材料裸露，接触表面出现点蚀和较大的剥落坑；最后，在接触应力的作用下产生大量塑性变形和疲劳裂纹，导致试样失效.

3 结论

a. 采用磁控溅射技术可以在GCr15马氏体钢表面沉积得到致密均匀的DLC薄膜，其硬度和弹性模量较高，且DLC薄膜与马氏体钢基体之间具有较高的界面结合强度.

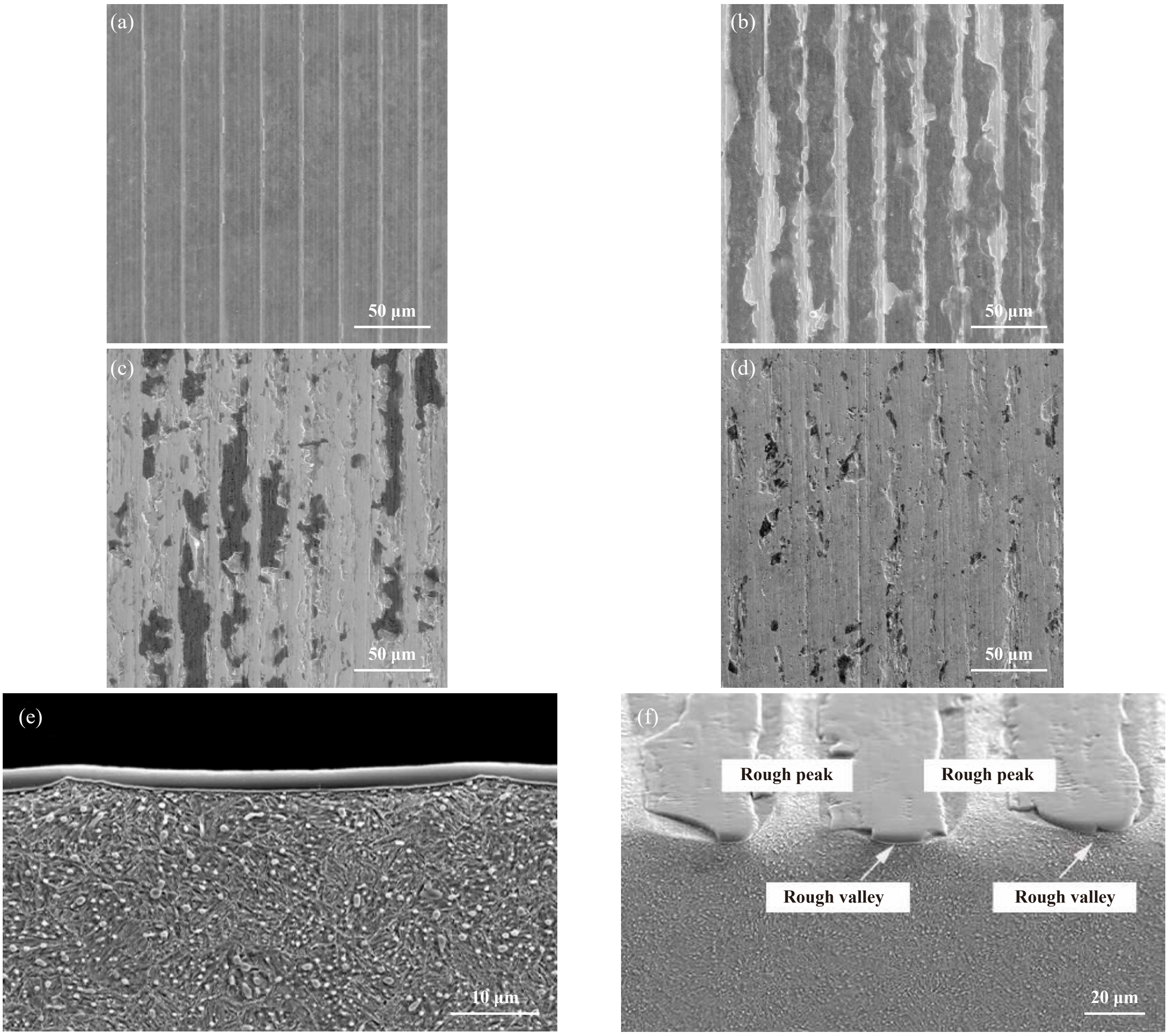

Fig. 8 SEM micrographs of DLC film samples: (a) surface before loading; (b) 3×10^4 cycles; (c) 1.2×10^5 cycles; (d) 1.8×10^5 cycles; (e) cross-section before loading; (f) cross-section of failed film sample

图 8　DLC薄膜试样SEM照片：(a) 加载前表面形貌；(b) 3×10^4周次；(c) 1.2×10^5周次；(d) 1.8×10^5周次；(e) 加载前截面形貌；(f) 薄膜试样失效截面形貌

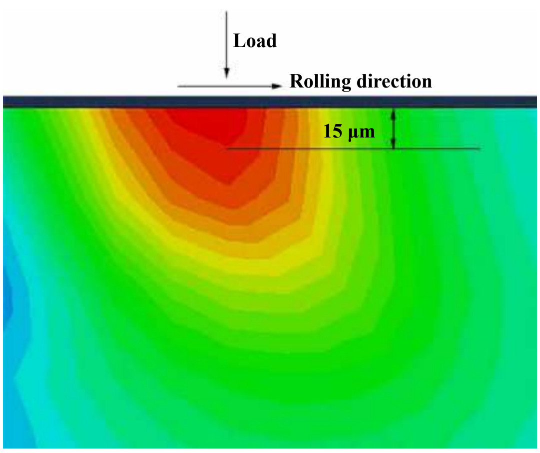

Fig. 9　Mises stress distribution of DLC film samples

图 9　DLC薄膜试样Mises应力等值曲线分布图

b. 与基体试样相比，DLC薄膜试样的接触疲劳寿命明显提高. 载荷和滑差率越大，寿命越短. 同时，DLC薄膜磨损完后的剩余寿命仍比原基体寿命长. 其原因一方面在于DLC薄膜本身的高硬度，另一方面由于DLC薄膜在滚动接触过程中形成了含碳转移膜，且转移膜具有石墨化特征，起到一定的润滑作用.

c. 薄膜试样滚动接触疲劳性能受基体表面粗糙峰和载荷条件等因素影响，其中表面粗糙峰影响最大. 薄膜厚度3 μm，处于接触最大应力分布的15 μm范围内. 在接触应力的作用下，微裂纹首先在基体表面的粗糙峰处产生，引起薄膜剥落并向四周扩展. 随着循环次数的增加，当薄膜磨完后，基体材料裸露，在疲劳

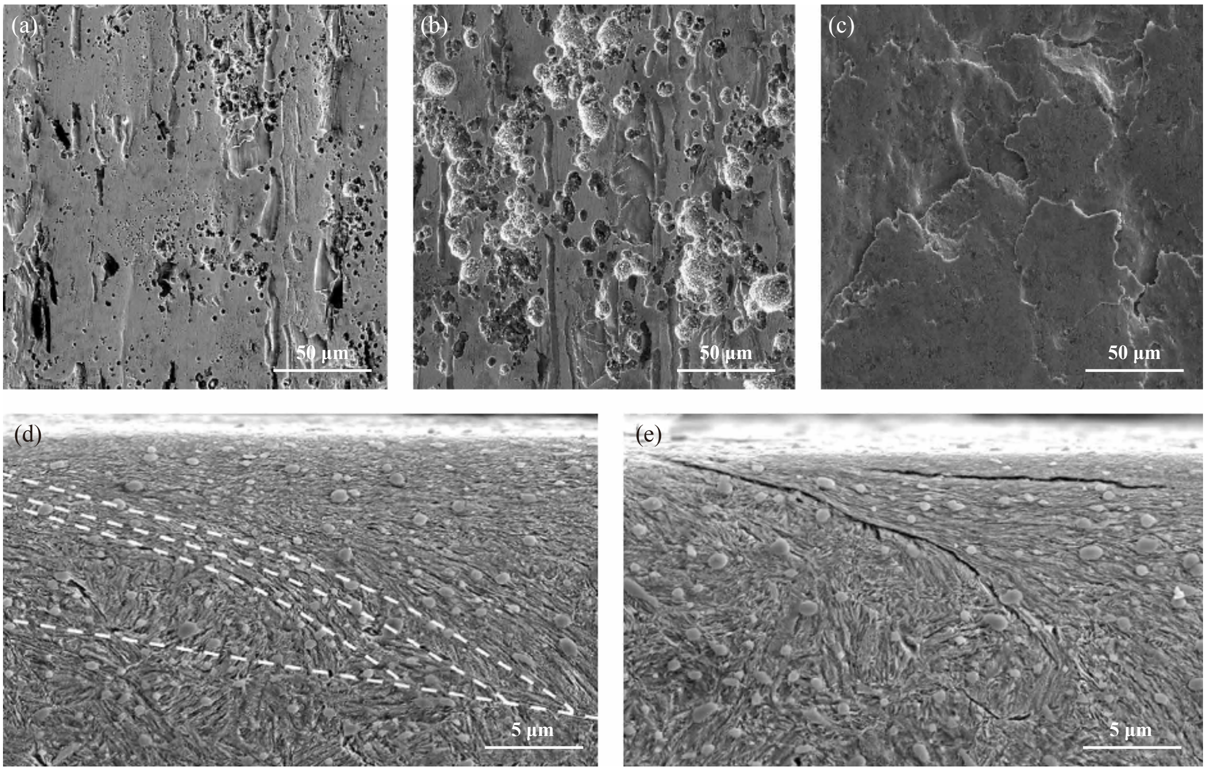

Fig. 10 SEM morphologies of the surface and across section microstructure of DLC film samples: (a~b) 1.8×10^5 cycles; (c) 3.4×10^6 cycles; (d~e) cross-section of failed film samples

图 10 DLC薄膜试样失效表面和横截面微观组织的SEM照片：(a~b)1.8×10^5周次；(c)3.4×10^6周次；(d~e)薄膜试样失效截面图像

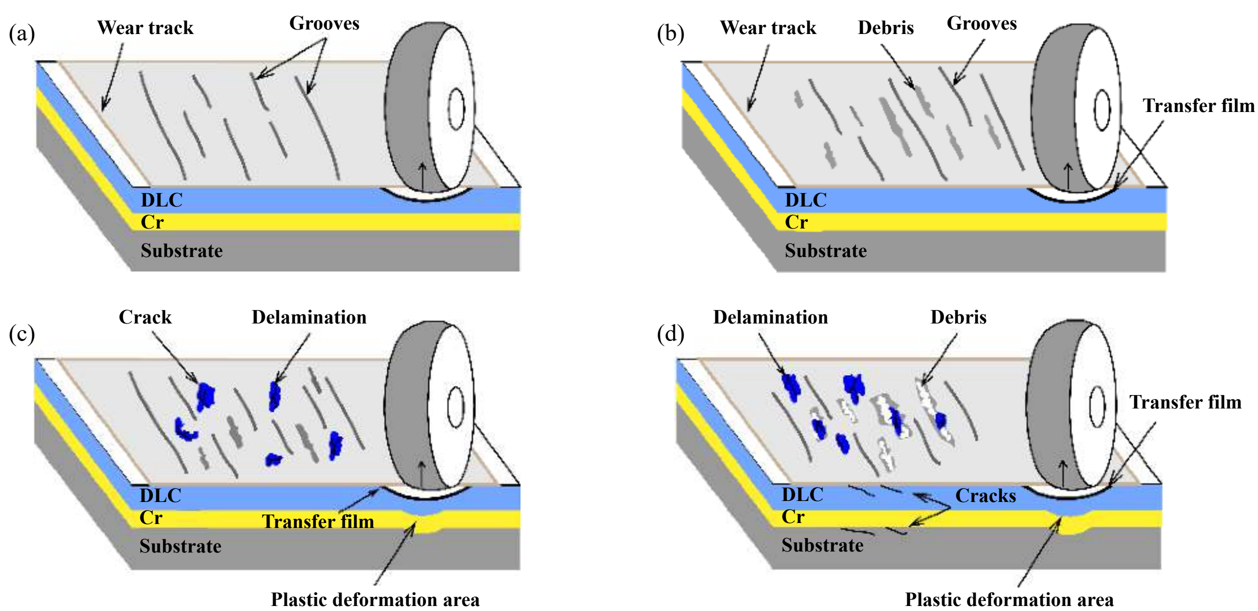

Fig. 11 Schematic diagrams of failure mechanism of DLC film samples

图 11 DLC薄膜试样失效机理示意图

载荷的作用下产生大量塑性变形和疲劳裂纹，最终导致试样失效.

参 考 文 献

[1] Evans H M. White structure flaking (WSF) in wind turbine gearbox bearings: effects of ‘butterflies’ and white etching cracks (WECs)[J]. Materials Science and Technology, 2012, 28(1): 3–22. doi: 10.1179/026708311X13135950699254.

[2] Liu Hongxi, Wang Langping, Wang Xiaofeng, et al. Effects of TiC films on the rolling contact fatigue life and mechanical properties of

bearing steel[J]. Acta Metallurgica Sinica, 2006, 42(11): 1197–1201 (in Chinese) [刘洪喜, 王浪平, 王小峰, 等. TiC薄膜对轴承钢表面滚动接触疲劳寿命和力学性能的影响[J]. 金属学报, 2006, 42(11): 1197–1201]. doi: 10.3321/j.issn:0412-1961.2006.11.015.

[3] Xue Qunji, Wang Liping. Diamond-like carbon based film material [M]. Beijing: Science Press, 2012 (in Chinese) [薛群基, 王立平. 类金刚石碳基薄膜材料[M]. 北京: 科学出版社, 2012].

[4] Zhang Junyan. Design and research advances of tribological films and coating[J]. Tribology, 2006, 26(4): 387–396 (in Chinese) [张俊彦. 薄膜/涂层的摩擦学设计及其研究进展[J]. 摩擦学学报, 2006, 26(4): 387–396]. doi: 10.3321/j.issn:1004-0595.2006.04.020.

[5] Chen Lin, Cao Xueqian, Lu Zhibin, et al. Improving the tribological properties of diamond-like carbon film applied under methane by tailoring sliding interface[J]. International Journal of Refractory Metals and Hard Materials, 2021, 94: 105380. doi: 10.1016/j.ijrmhm.2020.105380.

[6] Zhou Shengguo, Wang Liping, Xue Qunji. Effect of Al target power of magnetron sputtering on the structure and tribological properties of diamond-like carbon films[J]. Tribology, 2011, 31(3): 304–310 (in Chinese) [周升国, 王立平, 薛群基. 磁控溅射Al靶功率对类金刚石薄膜结构和摩擦学性能的影响[J]. 摩擦学学报, 2011, 31(3): 304–310]. doi: 10.16078/j.tribology.2011.03.008.

[7] Wang Dandan. Experimental assessment of the influence of DLC on contact fatigue capability of high-temperature bearing steel[D]. Harbin: Harbin Institute of Technology, 2018 (in Chinese) [王丹丹. DLC对高温轴承钢表面接触疲劳能力影响的试验评价[D]. 哈尔滨: 哈尔滨工业大学, 2018].

[8] Wu Xingyang, Chen Teng, Ge Zhou, et al. Tribological properties of N and Si Co-doped DLC films under different humidity conditions [J]. Tribology, 2017, 37(4): 501–509 (in Chinese) [吴行阳, 陈腾, 葛宙, 等. 不同湿度条件下N、Si共掺杂DLC膜的摩擦学性能研究[J]. 摩擦学学报, 2017, 37(4): 501–509]. doi: 10.16078/j.tribology.2017.04.012.

[9] Sui Xudong, Liu Jinyu, Zhang Shuaituo, et al. Microstructure, mechanical and tribological characterization of CrN/DLC/Cr-DLC multilayer coating with improved adhesive wear resistance[J]. Applied Surface Science, 2018, 439: 24–32. doi: 10.1016/j.apsusc.2017.12.266.

[10] Zhang Lili, Pu Jibin, Wang Liping, et al. Frictional dependence of graphene and carbon nanotube in diamond-like carbon/ionic liquids hybrid films in vacuum[J]. Carbon, 2014, 80: 734–745. doi: 10.1016/j.carbon.2014.09.022.

[11] Xu Wei, Dai Mingjiang, Lin Songsheng, et al. High temperature tribological behavior of W-doped diamond-like carbon films[J]. Tribology, 2017, 37(3): 379–386 (in Chinese) [许伟, 代明江, 林松盛, 等. 掺W类金刚石薄膜的高温摩擦学行为[J]. 摩擦学学报, 2017, 37(3): 379–386]. doi: 10.16078/j.tribology.2017.03.014.

[12] Wang Xiongwei, Chai Liqiang, Pang Xianjuan, et al. Influence of salt spray test to DLC film on tribological properties[J]. Tribology, 2018, 38(4): 453–461 (in Chinese) [王雄伟, 柴利强, 逄显娟, 等. 盐雾腐蚀对DLC薄膜摩擦学性能的影响[J]. 摩擦学学报, 2018, 38(4): 453–461]. doi: 10.16078/j.tribology.2018.04.010.

[13] Wei R H, Wilbur P J, Liston M J. Effects of diamond-like hydrocarbon films on rolling contact fatigue of bearing steels[J]. Diamond and Related Materials, 1993, 2(5-7): 898–903. doi: 10.1016/0925-9635(93)90247-Y.

[14] Rosado L, Jain V K, Trivedi H K. The effect of diamond-like carbon coatings on the rolling fatigue and wear of M50 steel[J]. Wear, 1997, 212(1): 1–6. doi: 10.1016/S0043-1648(97)00147-6.

[15] Xiao L, Rosen BG, Nilsson P H, et al. Rolling and rolling-to-sliding contact behaviour of DLC coatings[J]. Life Cycle Tribology, 2005, 48(5): 213–220. doi: 10.1016/s0167-8922(05)80023-9.

[16] Wei R H, Wilbur P J, Liston M J, et al. Rolling-contact-fatigue wear characteristics of diamond-like hydrocarbon coatings on steels[J]. Wear, 1993, 162–164(3): 558–568. doi:10.1016/0043-1648(93)90541-S. doi: 10.1016/0043-1648(93)90541-S.

[17] Li Shuxin, Su Yunshuai, Shu Xuedao, et al. Microstructural evolution in bearing steel under rolling contact fatigue[J]. wear, 2017, 380–381: 146–153. doi: 10.1016/j.wear.2017.03.018.

[18] Luo Qinghong, Zhao Zhenye, He Ziqiang, et al. Failure mechanism of contact fatigue of surface super-hardened M50NiL steel[J]. Journal of Aeronautical Materials, 2017, 37(6): 34–40 (in Chinese) [罗庆洪, 赵振业, 贺自强, 等. 表层超硬化M50NiL钢接触疲劳失效机理[J]. 航空材料学报, 2017, 37(6): 34–40]. doi: 10.11868/j.issn.1005-5053.2017.000108.

[19] Wang Junjun, Pu Jibin, Zhang Guangan, et al. Interface optimization and property investigation of DLC film with Si transition layer[J]. Tribology, 2014, 34(5): 531–537 (in Chinese) [王军军, 蒲吉斌, 张广安, 等. Si过渡层类金刚石薄膜界面优化及其性能研究[J]. 摩擦学学报, 2014, 34(5): 531–537]. doi: 10.16078/j.tribology.2014.05.008.

[20] Qian Jianguo, Li Shuxin, Pu Jibin, et al. Effect of heat treatment on structure and properties of molybdenum nitride and molybdenum carbonitride films prepared by magnetron sputtering[J]. Surface and Coatings Technology, 2019, 374: 725–735. doi: 10.1016/j.surfcoat.2019.06.062.

[21] Li Zhendong, Zhan Hua, Wang Yiqi, et al. Effect of substrate roughness on friction and wear properties of Cr-DLC films under dry-sliding condition[J]. Tribology, 2016, 36(6): 741–748 (in Chinese) [李振东, 詹华, 王亦奇, 等. 干摩擦条件下基体粗糙度对Cr-DLC薄膜摩擦磨损性能的影响[J]. 摩擦学学报, 2016, 36(6): 741–748]. doi: 10.16078/j.tribology.2016.06.011.

[22] Amanov A, Watabe T, Tsuboi R, et al. Fretting wear and fracture behaviors of Cr-doped and non-doped DLC films deposited on Ti-6Al-4V alloy by unbalanced magnetron sputtering[J]. Tribology International, 2013, 62: 49–57. doi: 10.1016/j.triboint.2013.01.020.

[23] Sun Lili, Dai Wei, Zhang Dong, et al. The effect of Cr-doped and Cr buffer layer on the adhesion of DLC film[J]. China Surface Engineering, 2010, 23(4): 26–28 (in Chinese) [孙丽丽, 代伟, 张栋, 等. Cr掺杂及Cr过渡层对类金刚石薄膜附着力的影响[J]. 中国表面

工程, 2010, 23(4): 26–28]. doi: 10.3969/j.issn.1007-9289.2010.04.006.

[24] Liu Hongxi, Jiang Yehua, Zhou Rong, et al. Effect of diamond-like carbon films on the bearing steel surface mechanical properties and rolling contact fatigue life[J]. Chinese Journal of Materials Research, 2009, 23(1): 43–48 (in Chinese) [刘洪喜, 蒋业华, 周荣, 等. 类金刚石薄膜对轴承钢表面机械性能和滚动接触疲劳寿命的影响[J]. 材料研究学报, 2009, 23(1): 43–48]. doi: 10.3321/j.issn:1005-3093.2009.01.009.

[25] Chen Lin, Wu Jian, Zhang Guangan, et al. Effect of interfacial control on tribological properties of diamond-like carbon based films in methane atmosphere[J]. Tribology, 2020, 40(2): 150–157 (in Chinese) [陈琳, 吴健, 张广安, 等. 界面调控对类金刚石碳基薄膜在甲烷气氛下摩擦学性能的影响[J]. 摩擦学学报, 2020, 40(2): 150–157]. doi: 10.16078/j.tribology.2019163.

[26] Ferrari A C, Robertson J. Interpretation of Raman spectra of disordered and amorphous carbon[J]. Physical Review B, 2000, 61(20): 14095–14107. doi: 10.1103/physrevb.61.14095.

[27] Manimunda P, Al-Azizi A, Kim S H, et al. Shear-induced structural changes and origin of ultralow friction of hydrogenated diamond-like carbon (DLC) in dry environment[J]. ACS Applied Materials & Interfaces, 2017, 9(19): 16704–16714. doi: 10.1021/acsami.7b03360.

[28] Chen Xinchun, Zhang Chenhui, Kato T, et al. Evolution of tribo-induced interfacial nanostructures governing superlubricity in a-C: H and a-C: H: Si films[J]. Nature Communications, 2017, 8(1): 1675. doi: 10.1038/s41467-017-01717-8.

[29] Sun Dong, Wang Haixin, Pu Jibin, et al. Application research of carbon-based films in aeroengine bearings under oil starvation condition[J]. Surface Technology, 2019, 48(8): 218–224 (in Chinese) [孙东, 王海新, 蒲吉斌, 等. 碳基薄膜在航空轴承乏油问题中的应用研究[J]. 表面技术, 2019, 48(8): 218–224]. doi: 10.16490/j.cnki.issn.1001-3660.2019.08.029.

[30] Fontaine J, Donnet C, Grill A, et al. Tribochemistry between hydrogen and diamond-like carbon films[J]. Surface and Coatings Technology, 2001, 146–147: 286–291. doi: 10.1016/S0257-8972(01)01398-6.

[31] Zhao Yiman, Liu Hongmei, Ji Li, et al. Effect of transfer film forming on super-low friction properties of hydrogenated amorphous carbon films[J]. Tribology, 2018, 38(1): 115–120 (in Chinese) [赵艺蔓, 刘红妹, 吉利, 等. 转移膜的形成对含氢碳膜超低摩擦性能的影响[J]. 摩擦学学报, 2018, 38(1): 115–120]. doi: 10.16078/j.tribology.2018.01.015.

[32] Erdemir A, Bindal C, Pagan J, et al. Characterization of transfer layers on steel surfaces sliding against diamond-like hydrocarbon films in dry nitrogen[J]. Surface and Coatings Technology, 1995, 76–77: 559–563. doi: 10.1016/0257-8972(95)02518-9.